INFORMATICA, 2004, Vol. 15, No. 4, 489–514

Moving Locally Predefined Remeshing for Deep Cone Penetration FE Analysis

Rimantas KAČIANAUSKAS, Darius MARKAUSKAS
Faculty of Fundamental Science, Vilnius Gediminas Technical University
Saulėtekio al. 11, LT-10223 Vilnius
e-mail: dm@fm.vtu.lt

Received: December 2004

Abstract. The paper considers moving locally predefined (MLP) finite element remeshing technique for deep penetration of the rigid cone into homogeneous and porous medium. Remeshing presents a computational tool implemented in the form of postprocessor type software compatible with standard FEM codes. It involves a transfer operation combining both the moving least square method based on stress patch recovery and the interpolation method for transfer of state variables. The developed MLP remeshing is able to overcome numerical difficulties occurring due to large distortions of the Lagrangian mesh and contact sliding and capture steady-state behavior. It shows good performance in modeling of cone penetration into elasto-plastic homogeneous and porous media reaching several diameters of the cone.

Key words: finite element method, moving locally predefined remeshing, deep cone penetration, saturated soil, elasto-plastic homogeneous medium, porous medium.

1. Introduction

Recently, the finite element method (FEM) has become a universal and powerful computational tool applied to many different problems of engineering analysis and has been a subject of an increasing amount of study for some time. The quality of numerical solutions depends, however, on the quality of the finite element mesh, where the appropriate meshing technique can considerably affect the final result. A complicated geometry and physics as well as a large amount of elements require the use of automatic meshing in order to considerably reduce the users' influence and the human errors in this process.

By now there has been a considerable effort devoted to the development of meshing and remeshing algorithms and software. The postprocessor type remeshing technique referred to as the adaptive FE analysis has been successfully used for the solution of linear elastostatic problems. Adaptive algorithms consist of building a new mesh, using the same type of elements, and 'adapting' the element size to the requirements of the solution. It means, reducing their size, when the interpolation must be enriched, i.e., higher accuracy is needed, and enlarging the elements, when it is already accurate enough. A remeshing technique is, actually, a computational tool giving the desired element size in the domain as a function of the pointwise error. An error assessment is needed to design

a new mesh verifying the accuracy prescription. The best mesh for a given FE analysis problem can be defined as a compromise between both the need for accurate results and the desire for computational efficiency. A consensus in terms of an optimal mesh is generally reached by combining the intelligent remeshing strategies and rigorous error estimation. Among numerous contributions, the works of Diez and Huerta (1999), Lee and Hoobs (1999), Owen and Saigal (2000), Baušys *et al*. (2001), Vasiliauskienė and Baušys (2002) illustrate the basic ideas of mesh adaptivity.

At present, the formal structure of the adaptive FE technique for linear elliptical problems is well known. This is not the case for non-stationary geometrical and, especially, structural non-linear problems, where the solution domain is undergoing considerable changes. However, due to large deformation in the process and the inherent nature of useful Lagrangian formulation with mesh nodes attached to material points, the finite element mesh distorts considerably. This leads to inaccuracies in computation of the state variables, numerical instability and inaccurate description of the deformed geometry, especially, contact geometry. Actually, the approximation of moving continuum by the time-dependent FE mesh presents two slightly different subproblems – generation of initial mesh and its adaptation in motion.

Perhaps the most general solution of a dynamic non-linear solid problem may be found in the framework of the Arbitrary Lagrangian Eulerian (ALE) formulation. A number of works of Belytschko and co-authors are reviewed in the book (Belytschko *et al.*, 2001) presenting a theory and some computational aspects of the FE ALE formulation. It describes both the motion of the material and the motion of the mesh, with mesh velocity being not equal to material velocity. Along with its versatility the ALE approach requires the evaluation of a new mesh in each time step and is quite expensive both in terms of solution effort and price of the software codes. Meshing problems related to different formulations have been discussed by Chenot and Bay (1998).

In terms of the conventional Lagrangian formulation traditionally used in mechanics of solids and a wide range of engineering applications, the mesh distortion problem can be resolved with a proper remeshing technique. In this case, a solution procedure cannot be repeated from the initial configuration, but has to be continued from the previously computed state. The basic idea of *advanced remeshing* is to ensure discretisation of the current deformed configuration, with all history-dependent variables being transferred from the reference mesh to the new deformed mesh. It comprises a loop of operations until the required accuracy has been reached and requires a decision making mechanism for remeshing. The remeshing concept in the Lagrangian framework will be kept in mind throughout the paper, avoiding discussion about the formulation which would make the paper overlong and go beyond the scope of the paper. In addition, it would be quite natural for dealing with porous media as it has been used in various applications.

The potential areas of engineering applications driving the development of the FE remeshing technique mainly concern metal forming (Zhu *et al*., 1997; Chand and Kumar, 1998; Liu *et al*., 1998; Alves *et al*., 2003; Gautham *et al.*, 2003) and fracture mechanics (Bouchard *et al*., 2003; Yang and Chen, 2004).

The use of remeshing in other engineering areas, including geotechnical problems, is still limited. The applications concern standard problems such as bearing capacity anal-

ysis of strip and circular foundations (Hu and Randolph, 1998) and pile driving (Liyanapathirana *et al*., 2000). One of the most challenging issues in geotechnical engineering is simulation of cone penetrations tests (CPT) used to evaluate in-situ properties of soil, since the cone must be pushed into soil with a vertical displacement several times the diameter of the cone. However, a large distortion of the finite element geometry during penetration leading to ill-conditioned equations and failure of an iterative process restricted the application of the FEM to CPT modeling. Recently, remeshing as an alternative to avoid a large mesh distortion has been applied for these purposes (Markauskas *et al*., 2003; Susila and Hryciw, 2003).

Up to now, all the above mentioned applications of remeshing have been limited to modeling the solution domain as a single field medium. However, most of the problems are really multi-physics problems, where coupling of different field variables has to be taken into account. Remeshing issues with respect to the coupled thermo-mechanical problems and related to metal forming problems are reported by Lee *et al*. (2002) and by Wriggers and Rieger (2003), while penetration into the porous medium with remeshing described in terms of the coupled solid-pore water model is presented by Markauskas (2003).

An advanced FE remeshing technique comprises both the theoretical and algorithmic aspects. Theoretical aspects are mainly related to quality of mesh to be continuously monitored during the entire simulation process, where error estimation procedures play a crucial role. Different universal and problem-oriented error estimators based on the error norm of stress, strains or energy as well as different error indicators frequently used in adaptive FE analysis (Zienkiewicz and Zhu, 1992; Hu and Randolph, 1998; Diez and Huerta, 1999; Baušys *et al*., 2001; Gautham *et al*., 2003) may be explored for these purposes.

Besides the above error-based criteria on element size distribution, it would be also necessary to have a geometrically based measure of the deformation of the mesh characterising the geometric distortion of the elements (Zhu *et al*., 1997; Liu *et al*., 1998; Gautham *et al*., 2003; Alves *et al*., 2003). The majority of these are based on geometric metrics such as aspect ratio, diagonal ratio, skew, taper, etc. Theoretical aspects related to a specific remeshing issue, namely, the variable transfer operation between meshes, seems to be originally generalised by Peric *et al*. (1996).

The geometric measures, however, cannot capture all difficulties associated with the description of geometry in the case of contact problems. When the contact boundary is not exactly recovered, the geometry errors provide artificial shocks of contact forces destroying monotonic convergence of the iterative process. The theoretical solution of this problem has not been known until now, while in engineering applications the problem is being solved in an algorithmic way combining the theoretical knowledge with the heuristic and semi-empirical arguments.

Now, the number of studies devoted to algorithmic aspects of the remeshing technique are growing fast. In this respect, it can be stated that a considerable effort is focused on the development and improvement of the meshing and remeshing codes in different fields. On the other hand, the most popular universal and problem oriented FE codes used in

research and industry are seldom supported with the remeshing utilities, although many details of the algorithms are not available for commercial reasons.

The algorithmic issues mainly comprise the choice of elements, remeshing strategies, mesh generation technique and data transfer between different meshes. The most commonly used finite elements for the simulation of 2D problems are linear or quadrilateral elements. The application of the constant stress triangle is limited by its insufficient accuracy, though the generation of mesh is considerably easier (Peric *et al*., 1996; Bouchard *et al*., 2003). The latest advantage has been extensively explored in the adaptive remeshing by applying six-node triangular elements (Hu and Randolph, 1998). However, the quadrilateral elements forming the basis of structured meshes have not received due attention in remeshing procedures. This could be accounted for the difficulties in generating unstructured all-quadrilateral meshes. The remeshing algorithms with four-node quadrilateral mesh generators for the 2D metal forming problems are demonstrated by Gautham *et al.* (2003) and by Chand and Kumar (1998). In the case of remeshing for a large deformation analysis, eight-node elements might be preferable (Zhu *et al*., 1997; Pedersen, 1998). In recent years, a great effort has been made in developing three-dimensional remeshing algorithms (Lee *et al*., 2002; Alves *et al*., 2003), where the discussion around the choice between tetrahedral and hexahedral elements is still continued.

The aim of remeshing is to provide a proper discretisation tool to continue simulation for the whole structure deformation period. This aim may be achieved by implementing the corresponding remeshing strategy to be addressed in this discussion. In general, *adaptive* remeshing with an adaptive mesh perfectly fitting the deformed geometry at any time increment may be considered the most perfect modelling strategy. The generation of a new mesh is required, when a number of elements may get excessively distorted outside the quality limits. Here, any element and time step size have to be automatically adjusted according to given criteria. Examples of the particular problem-oriented adaptive remeshing are presented by Zhu *et al*. (1997), Bouchard *et al*. (2003) and Gautham *et al*. (2003).

In adaptive remeshing applications, the number of elements is typically increased, when a mesh is renewed. Frequent adaptive remeshing, however, results in an increase in both the cost and the error of computation. In order to control the total model size, *constant mesh-structural topology* strategy is used as an alternative. This alternative is based on the concept of a background mesh. The background mesh can move with the deformed domain geometry. In most cases, the background mesh is a structured mesh, whereas the available elements are concentrated in the areas of the model, where the largest stress and strain gradients occur.

Generally, mesh distortion may have a global or local nature. In the case when the average mesh quality is outside the limits, the *globally* predefined remeshing procedure with recalculation of new positions of the nodes is employed. The location of new nodes is obtained by sweeping the mesh according to global changes of the entire structure (Chand and Kumar, 1998; Pedersen, 1998; Lee *et al*., 2002).

Otherwise, the strain and stress often concentrate in some locations within the solution domain. They may occur in interfering with the rigid boundary as in metal forming (Liu

et al., 1998; Gautham *et al.*, 2003) and penetration problems (Markauskas, 2003) or in the propagation of locally embedded cracks during fracture (Bouchard *et al.*, 2003). Therefore, only a few elements cause a severe distortion, while the remaining elements are deformed slightly. The local distortion may be avoided in two ways. Firstly, *local* readjustment may be done by generating a new mesh having a new topology with special attention to a local subregion, for example, in the vicinity of the crack tip (Yang and Chen, 2004). Secondly, the *locally predefined* strategy is that the elements in a new mesh retain after remeshing the same mesh-structural topology as the old one. Some examples of local remeshing in metal forming are presented by Liu *et al*. (1998). Actually, different combinations of remeshing strategies supplied by different error and distortion measures can raise the efficiency of the FE simulation.

Another most important issue in remeshing is the transfer of the state variables between old and new meshes during an incremental transient or non-linear process. Since mapping cannot be supplemented with equilibrium iterations, mapping errors may propagate and pollute the whole simulation. Two basic mapping methods have been evaluated. The intra/extrapolation method using conventional FE shape functions is applied mainly for the transfer of nodal values of primary state variables such as displacements or pressures (Peric *et al.*, 1996; Alves *et al.*, 2003), while a moving least square method is applied to the transfer of the values of secondary state variables such as stress, strains, internal variables, etc., defined in Gauss integration points (Chand and Kumar, 1998). A combination of both methods is also possible (Pedersen, 1998; Zhu *et al.*, 1997).

The paper addresses the moving locally predefined FE remeshing technique for deep penetration of the rigid cone into deformable medium. Remeshing techique presents a problem-orented computational tool implemented in the form of the postprocessor type software compatible with standard FEM codes. A major goal is to illustrate the capability of the developed technique to capture steady state penetration of the cone into the porous media with penetration depth of several diameters, which is still a very difficult or even insolvable problem using standard FE software.

The paper is organized as follows. In Section 2, the cone penetration problem and the main solution issues are described. The coupled two-field FE model with remeshing for the non-linear elasto-plastic porous medium are presented in Section 3. The proposed moving locally predefined FE remeshing technique involving the transfer of the state variables is reported in Section 4. Finally, the numerical performance of remeshing by the investigation of penetration into homogeneous and porous media is illustrated and a discussion on the results is reported in Section 5.

2. Problem Description

The cone penetration test is an effective experimental tool to evaluate in-situ properties of the soil which is extensively used in geotechnical engineering. One of the primary applications of these tests was to measure the cone resistance. Advanced devices also involve measurements of the friction along the sleeve of the tool and the pore pressure at different locations.

Actually, the most important characteristic relating to experimental measurements and mechanical properties of the medium is cone resistance which has to be obtained by deep steady-state penetration. It presents the acting resultant force on the cone tip divided by the cone cross area. Typically, the whole penetration procedure follows from several to dozens of meters.

The experimental device referred to as penetrometer presents a cone on the end of a series of rods. It is pushed into the deformable medium at a constant rate. The cone with a diameter d of 35.7 mm, cone tip angle – 60° and penetration speed equal to 2 cm/s is usually referred to as a standard one (Lunne *et al.*, 1997).

Nowadays, most of the efforts of engineers are focused, however, on the correlation and correction of measurement results, rather than physical interpretation of factors influencing the stress and pressure fields around the cone. An efficient way of interpreting cone-soil interaction is numerical modeling. The finite element method widely used in engineering alongside the existing semi-empirical approaches, becomes the most attractive alternative to handle the penetration problem and the influence of various factors on cone resistance.

In the numerical simulations, the penetrometer is considered to be a rigid cone pre-embedded into a hole pre-bored in deformable half-space medium (Fig. 1). The penetration process is initiated by applying displacement u to the rigid surface of the penetrometer, until a steady state is reached. The numerically obtained loading curve relating to the resultant load F acting on the tip of the cone and cone displacement u are the most important characteristics of the resistance and, at the same time, the quality indicator of numerical analysis. Actually, to capture the steady-state behavior and cone resistance of soil, the cone must be pushed into the medium at the depth of several diameters of the cone.

Since the cone is penetrating by vertical loading, the 3D problem may be reduced to axi-symmetric one with 2D domain (Fig. 2). To avoid boundary effects at the start of the analysis, the cone is placed into a pre-bored hole having the initial depth h, with the surrounding soil still in its in-situ stress state.

The soil region divided by finite elements should be considerably large to avoid the influence on the result of the replacement of the infinite half-space by a limited size

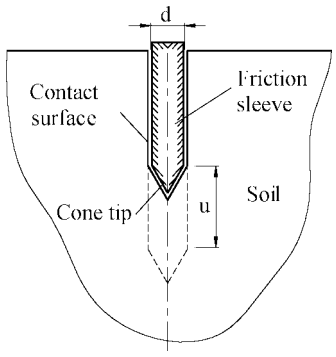

Fig. 1. Illustration of cone penetration.

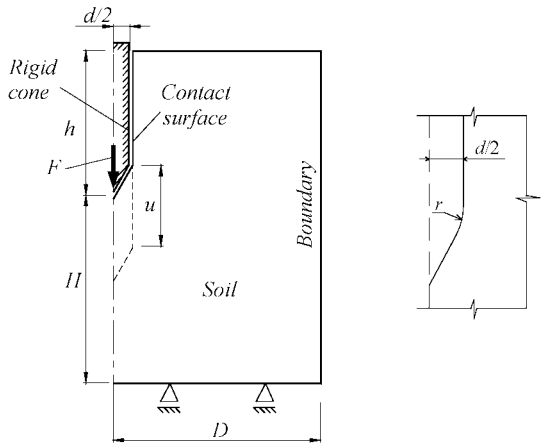

Fig. 2. 2D solution domain (a) and the smoothed geometry of penetrometer (b).

zone. The size of the 2D solution domain is defined by two parameters, D and $h + H$, the values of which are usually verified by numerical experiments with a larger domain. The symmetry axis and the bottom boundary are assumed to be rigid, while the right boundary reflects the external surrounding infinity medium, where boundary conditions may be prescribed by using a rigid surface or infinite elements.

The nature of the penetration problem is highly non-linear, while the main difficulties are referred not only to large strain and material non-linearities governed by continuum mechanics equations, but also to considerable changes of geometry of solution domain and mainly, as a consequence, to contact sliding. The reliable response calculation requires, however, the proper choice of the FE discretisation as well as mathematical problem formulation.

Up to now, all known FE applications to cone penetration problem were performed using the structured quadrilateral mesh. The arguments to prefer this meshing strategy to a popular adaptive approach may be explained as follows. The problem contains two concentrators, the cone tip and sharp connection of the cone and the sleeve. A traditional procedure of the adaptive finite element refinement leads even to a larger local distortion of mesh in the vicinity of the concentrators, and, as a consequence, the simulation process of penetration fails at smaller displacement values. To avoid such a large mesh distortion, larger elements can be used (Sheng *et al.*, 1997; Mabsout *et al.*, 1995), but, in this case, the accuracy of calculated stress values decreases dramatically. Difficulties of another type, apart from FE mesh, are associated with the conventional displacement approach and Lagrangian type problem formulation for a single constant topology mesh. It was pointed out by van den Berg (1994) and later reported by Song *et al.* (1999), Markauskas *et al.* (2002) and Voyiadjis and Kim (2003). Large distortions of the finite element geometry during penetration leading to the failure of an implicit iterative solution schema restricted the application of the FEM to CPT modeling. Probably the most successful latest results of this kind, with application to porous medium, were reported by Voyiadjis and Kim

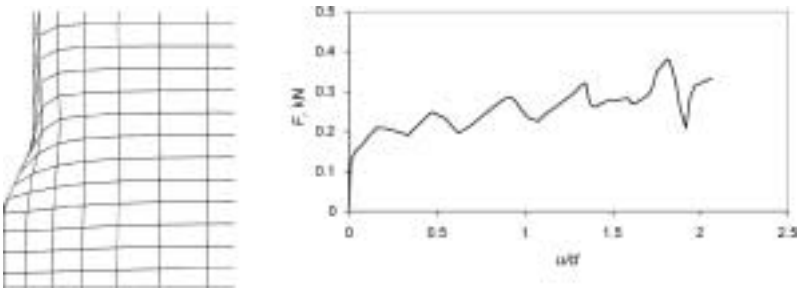

Fig. 3. Results of CPT analysis without remeshing: a) deformed geometry, b) loading curve.

(2003). They were related, however, not to a standard but to mini cone and were limited by penetration depth of 3.5 diameter of the cone.

The interpretation of the local behaviour (Markauskas *et al.*, 2003) illustrates that not only distortion, but contact sliding play a crucial role. By sliding of the cone with respect to a solid, the outer contact solid node after a certain period of relatively slow sliding loses the contact with the conical surface of the cone and moves along the vertical surface of the sleeve at a higher rate.

To illustrate the arising difficulties, cone penetration analysis with contact behaviour is considered using a smooth cone with smoothed geometry (Fig. 2b), where a sharp cone-sleeve connection is approximated by a circular curve with the rounded-off radius r. Numerical results obtained for the cone with $r = 10$ mm presented in Fig. 3 are a typical illustration of the cone behaviour. As follows from a simple observation, a large distortion of mesh (Fig. 3a) and the irregular character of a loading curve (Fig. 3b) leading to the failure of computation process at relatively small displacement values clearly indicate unsatisfactory validity of numerical simulation. In this case, the corner node criterion value (Erhart *et al.*, 2001) is below 0, which indicates that an element is irregular. By using a smaller value of the rounded radius, finally tending to the sharp angle, and by including the increasing roughness of contact, this tendency is even worse.

Finally, the above drawbacks show that a single mesh strategy is not able to follow deep penetration, therefore, new innovative meshing strategies are required, one of which is expected to be moving locally predefined remeshing.

3. Mathematical Models

The deformable medium penetrated is expected to be a soil which consists of solid grain particles and voids that are filled with water and/or air. Generally, the soil presents a mixture, the behaviour of which may be described by a mathematical model of multi-phase deformable medium.

In the framework of the current investigation, deformable medium is considered to be the two-phase porous medium consisting of solid grains (skeleton) and pore water. Each phase is regarded as individual continuum following its own behavior governed

by different equations. The skeleton is assumed to be elastic-plastic solid undergoing large strains and large displacements, while the flow of pore-water through the voids is assumed to follow Darcy's law. Under certain assumptions, the flow of pore-water may be neglected and two-phase medium model may be transformed to homogeneous continuum model.

A mathematical model explored here to describe the medium is a widely used Lagrangian continuum mechanics approach with respect to remeshing. It is based on the equilibrium of internal and external virtual works in the current configuration corresponding to time $t + \Delta t$ and should be written for the current volume ${}^{t+\Delta t}V$ as:

$$\int\limits_{{}^{t+\Delta t}V} {}^{t+\Delta t}\tau_{ij} \cdot \delta^{t+\Delta t} e_{ij} \, {}^{t+\Delta t}\mathrm{d}\, V = \delta^{t+\Delta t} R, \tag{1}$$

where ${}^{t+\Delta t}\tau_{ij}$ are the Cartesian components of the Cauchy stress tensor, ${}^{t+\Delta t}e_{ij}$ are the Cartesian components of an infinitesimal strain tensor and $\delta^{t+\Delta t}R$ is the virtual external work. The t denotes time related to reference configuration, while Δt stands for time operation interval. It is not related to time step associated with the appropriate numerical incremental procedure. Such interpretation reflects the essence of the developed remeshing technique and enables us to omit a discussion concerning the computational aspects of the total and the updated Lagrangian formulations.

Here and further, the left-side superscript indicates the configuration related to time t in which the quantity occurs, while the left-side subscript indicates the configuration in which the quantity is measured. If the quantity occurs in the same configuration in which it is also measures, the left subscript may be omitted, e.g., we may have ${}^{t+\Delta t}\tau_{ij} \equiv {}^{t+\Delta t}_{t+\Delta t}\tau_{ij}$.

The body is described by a non-linear constitutive relationship as well by non-linear contact boundary conditions, but since it also undergoes large displacements and large strains causing the unknown current configurations, the relation in (1) cannot be solved directly. In spite of certain differences occurring in interpreting the Lagrangian approach (Bathe, 1982; Crisfield, 1997; Belytschko *et al.*, 2001) all of the studies define stress and strain measures referred to the reference configuration corresponding to time t:

In addition, the behavior of porous solid is also affected by pressure p of pore-water filling the voids, and the concept of effective stress is employed to describe the effect of strong coupling, where conventional Cauchy stress tensor ${}^{t}\tau_{ij}$ is replaced by the effective Cauchy stress tensor ${}^{t}\tau'_{ij}$ such that

$${}^{t}\tau'_{ij} = {}^{t}\tau_{ij} + {}^{t}p\delta_{ij}, \tag{2}$$

where δ_{ij} is Kronecker delta.

The coupled soil-pore fluid model of porous medium presents the equilibrium equations of the skeleton-fluid mixture which can be written using the principle of virtual work (1) with respect to (2) and the balance of mass, which simply means a transient seepage equation. By considering saturated incompressible medium and omitting the details, it

may be sufficient to consider a general matrix form of coupled transient static finite element equations, expressed in terms of the nodal displacements $\{\boldsymbol{u}\}$, nodal pressures $\{\boldsymbol{p}\}$ and their velocities $\{\dot{\boldsymbol{u}}\}$ and $\{\dot{\boldsymbol{p}}\}$ (Zienkiewicz, 1984):

$$\begin{bmatrix} \boldsymbol{0} & \boldsymbol{0} \\ -\boldsymbol{Q}^{\mathrm{T}} & \boldsymbol{0} \end{bmatrix} \begin{Bmatrix} \dot{\boldsymbol{u}}(t) \\ \dot{\boldsymbol{p}}(t) \end{Bmatrix} + \begin{bmatrix} \boldsymbol{K} & \boldsymbol{Q} \\ \boldsymbol{0} & \boldsymbol{H} \end{bmatrix} \begin{Bmatrix} \boldsymbol{u}(t) \\ \boldsymbol{p}(t) \end{Bmatrix} = - \begin{Bmatrix} \boldsymbol{F}(t) \\ \boldsymbol{q}(t) \end{Bmatrix}. \tag{3}$$

Here, $[\boldsymbol{K}]$ presents the structural stiffness matrix, and the fluid matrix $[\boldsymbol{H}]$ presents permeability, while $[\boldsymbol{Q}]$ couples the field of pressures in the equilibrium equations. The right-hand vector stands for external forces and flows $\{\boldsymbol{F}\}$ and $\{\boldsymbol{q}\}$ including boundary terms.

The incremental Lagrangian FE formulation of coupled equations (3) may be presented as follows (see for example Voyiadjis and Abu-Farsakh, 1997; Potts and Zdravkovic, 1999):

$$\begin{bmatrix} {}^{t}\boldsymbol{K} & {}^{t}\boldsymbol{Q} \\ -{}^{t}\boldsymbol{Q}^{\mathrm{T}} & {}^{t}\boldsymbol{H}\Delta t \end{bmatrix} \begin{Bmatrix} {}^{t}\Delta\boldsymbol{u} \\ {}^{t}\Delta\boldsymbol{p} \end{Bmatrix} = - \begin{Bmatrix} {}^{t}\Delta\boldsymbol{F} \\ {}^{t}\Delta\boldsymbol{q} \end{Bmatrix}. \tag{4}$$

Here, $\{{}^{t}\Delta\boldsymbol{u}\}$ and $\{{}^{t}\Delta\boldsymbol{p}\}$ are increments of the nodal displacements and pressures during time operation interval Δt, $[{}^{t}\boldsymbol{K}]$, $[{}^{t}\boldsymbol{Q}]$ and $[{}^{t}\boldsymbol{H}]$ presents the coefficient matrices defined in configuration t, while $\{{}^{t}\Delta\boldsymbol{F}\}$ and $\{{}^{t}\Delta\boldsymbol{q}\}$ are increments of the external nodal load and flow, respectively.

Increments of the nodal variables for the time interval Δt are defined in a usual manner as $\{{}^{t}\Delta\boldsymbol{u}\} = \{{}^{t+\Delta t}\boldsymbol{u}\} - \{{}^{t}\boldsymbol{u}\}$.

The original formulation (3)–(4) assumes the single initial finite element mesh defined for the entire operation interval. Let us denote values of the scalars, vectors and matrices at time t related to the mesh h by the right-side subscript h.

As it is obviously used in the finite element method, a discussion on the matrices of (4) will be continued for an individual element e denoted hereafter by the right-side superscript e. Let us consider mesh h, defined in reference configuration t. For the sake of simplicity, the incremental stiffness matrix may be presented in two terms:

$$\begin{aligned} [{}^{t}\boldsymbol{K}_{h}^{e}] = & \int\limits_{{}^{t}V_{h}^{e}} [{}^{t}\boldsymbol{B}_{h}^{e}]^{\mathrm{T}} \left[{}^{t}\boldsymbol{C}^{ep}({}^{t}\chi_{h}^{e})\right] [{}^{t}\boldsymbol{B}_{h}^{e}] {}^{t}\mathrm{d}\,V \\ & + \int\limits_{{}^{t}V_{h}^{e}} [{}^{t}\boldsymbol{B}_{NLh}^{e}]^{\mathrm{T}} [{}^{t}\boldsymbol{\tau}_{h}^{e}] [{}^{t}\boldsymbol{B}_{NLh}^{e}] {}^{t}\mathrm{d}\,V. \end{aligned} \tag{5}$$

Here, the integration is performed in the reference volume ${}^{t}V_{h}^{e}$ defined in mesh h. The first term expresses the conventional stiffness $[{}^{t}\boldsymbol{K}^{e}]$ including initial displacements, while the second term $[{}^{t}\boldsymbol{K}_{G}^{e}]$ denotes the geometric stiffness matrices. Here, $[{}^{t}\boldsymbol{B}^{e}] = [{}^{t}\boldsymbol{B}_{L}^{e}] + [{}^{t}\boldsymbol{B}_{NL}^{e}]$ is the non-linear strain-displacement transformation matrix for the total strain composed of the linear and non-linear terms $[{}^{t}\boldsymbol{B}_{L}^{e}]$ and $[{}^{t}\boldsymbol{B}_{NL}^{e}]$, respectively. $[{}^{t}\boldsymbol{C}^{ep}]$ is the elastoplastic material property matrix depending on the internal

variable ${}^t\chi^e$, which, in our case, is a history-dependent hardening parameter, while matrix $[{}^t\boldsymbol{\tau}]$ stands for Cauchy stresses. The contact boundary conditions between the deformable medium and the rigid cone surface may be also implemented in different ways. The kinematic measures of overclosure and of relative shear sliding are controlled at each prescribed integration point. They have to be obtained in the same manner as the stiffness matrix (5). The remaining matrices $[{}^t\boldsymbol{Q}_h^e]$ and $[{}^t\boldsymbol{H}_h^e]$ are defined in a similar manner.

The given incremental right hand vectors $\{{}^t\Delta\boldsymbol{F}_h^e\}$ and $\{{}^t\Delta\boldsymbol{q}_h^e\}$ are defined in a similar way. The load vector $\{{}^t\Delta\boldsymbol{F}_h^e\}$ is presented as follows:

$$\{{}^t\Delta\boldsymbol{F}_h^e\} = \{{}^{t+\Delta t}\boldsymbol{F}_h^e\} - \int\limits_{{}^tV_h^e} [{}^t\boldsymbol{B}_{Lh}^e]^T [{}^t\boldsymbol{\tau}_h^e]^t \mathrm{d}\, V. \tag{6}$$

Here, $\{{}^{t+\Delta t}\boldsymbol{F}^e\}$ is the vector of the external applied nodal loads at time $t+\Delta t$ incorporating body forces and tractions, while the second term presents the resultant nodal forces due to element stresses at time t.

At a certain time instance *tr*, when the current configuration undergoes considerable changes distorting initial mesh h defined at reference configuration t, a new mesh should be generated. By applying the remeshing technique, the incremental equation (4) and the corresponding matrices must be reformulated in the new mesh $h+1$, while the solution procedure has to be continued from the previously computed state related to the mesh h.

Now, the stiffness matrix (6) has to be defined as

$$\begin{aligned}[{}^{tr}\boldsymbol{K}_{h+1}^e] = &\int\limits_{{}^{tr}V_{h+1}^e} [{}^{tr}\boldsymbol{B}_{h+1}^e]^{\mathrm{T}} \big[{}^{tr}\boldsymbol{C}^{ep}({}^{tr}\chi_{h+1}^e)\big] [{}^{tr}\boldsymbol{B}_{h+1}^e]^{tr}\mathrm{d}\, V \\ &+ \int\limits_{{}^{rt}V_{h+1}^e} [{}^{tr}\boldsymbol{B}_{NLh+1}^e]^{\mathrm{T}} [{}^{tr}\boldsymbol{\tau}_{h+1}^e] [{}^{tr}\boldsymbol{B}_{NLh+1}^e]^{tr}\mathrm{d}\, V.\end{aligned} \tag{7}$$

Computation of the new matrix (7) may be implemented in different ways. The current development is aimed at keeping to standard procedures as much as possible. The integration methodology over the deformed domain is, generally, mesh independent. Since the new material property matrix $[{}^{tr}\boldsymbol{C}^{ep}]$ and geometric matrices $[{}^{tr}\boldsymbol{B}_{h+1}^e]$ and $[{}^{tr}\boldsymbol{B}_{NLh+1}^e]$ may be calculated in the new mesh geometry using the same procedures of standard codes, the main difference occurs by imposing the values of the Cauchy stress $\{{}^{tr}\boldsymbol{\tau}_{h+1}^e\}$ and hardening parameter ${}^{tr}\chi_{h+1}^e$. These values have to be transferred from the old mesh h to the new mesh $h+1$. Reformulation of other matrices and vectors in the new mesh $h+1$ may be done in a similar way as in the case of the stiffness matrix (5). The main difference is that, in addition to Cauchy stress and hardening parameter, the values of pore-water pressure $\{{}^t\boldsymbol{p}_h\}$ obtained in the mesh h have to be transferred to the new mesh $h+1$ as $\{{}^{tr}\boldsymbol{p}_{h+1}\}$. The transfer operation belongs to the remeshing technique to be implemented.

Homogeneous solid presents a particular case of the model (4).

4. Remeshing Technique

The proposed and developed remeshing technique presents a problem-oriented technique devoted to simulation of deep penetration into deformable homogeneous and porous medium. Generally, the remeshing technique comprises three phases. First, an initial or background mesh must be chosen. Next, guidelines for the generation of the new mesh (remeshing decision and new mesh generation) are required and, finally, a procedure for the transfer of data between the meshes has to be developed.

The initial mesh is assumed to be a background mesh. Its generation takes into account the experience gained by the authors and other researchers. It presents a structured quadrilateral mesh with four-node bilinear isoparametric elements with full integration for displacement and pore pressure fields. They are quite simple for the generation purpose, as well as preventing mesh locking and may be applied for both homogeneous and porous media. The four Gauss integration points allow us to recover the variation of the internal variables in the new mesh with sufficient accuracy. The mesh density has a locally predefined character since the highest stress and strain gradients occur in the vicinity of the contact zone between the rigid cone and deformable medium. The critical element size is chosen a priory along the contact cone surface. This refinement is swept into both directions, thereby covering the entire solution domain and fitting requirements of relative element sides.

The moving strategy is chosen for remeshing. The local background mesh with constant characteristic size a remains unchanged during the entire operation period. Its location is predefined by the location of the moving cone. Because penetration actually presents the motion of the cone, driven by displacement increments Δu, the mesh is regenerated at the prescribed increments. At each increment the new global mesh is then generated according to the requirements used in the generation of the background mesh. The concept of the moving locally predefined (MLP) remeshing is illustrated in Fig. 4.

Most of different remeshing criteria found in the literature are based on geometrical or local error observations. In our problem, the critical distortion occurs at the cone-sleeve connection. It makes the deformation process irregular, but the main reason for this is not only the distorted geometry, but the sliding of the element with respect to the

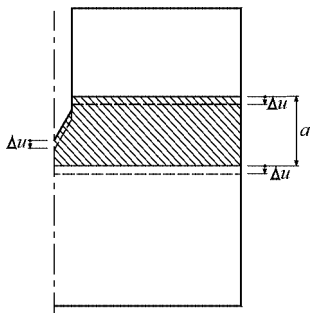

Fig. 4. Illustration of strategy of the moving locally predefined remeshing.

corner node. To prevent sudden jumping of the element node from the conical surface of the cone, which leads to very slow convergence of the equilibrium when using an implicit time integration schema, a regular remeshing frequency with the predefined displacement increment Δu equal $l/2$ to l, where l is the size of the smallest element, was put forward as a remeshing indicator.

The remeshing is supplied with a transfer operation of the required state variables. The coupled model (4) contains two types of internal variables, which have to be transferred to a new mesh. The pressure field $\{\boldsymbol{p}\}$ is described by primary variables defined at nodes, while the stress field described by Cauchy stress $\{\boldsymbol{\tau}\}$ and internal variables presenting hardening parameter χ are defined at Gauss points, therefore, a combined transfer technique with two different procedures has to be used.

The transfer operation at time instance *tr* between the new mesh $h+1$ and the old mesh h is presented here by linear transformations. For Cauchy stress

$$\{{}^{tr}\boldsymbol{\tau}_{h+1}\} = [\boldsymbol{T}_s]\{{}^{tr}\boldsymbol{\tau}_h\}, \tag{8}$$

while for pore pressure

$$\{{}^{tr}\boldsymbol{p}_{h+1}\} = [\boldsymbol{T}_p]\{{}^{tr}\boldsymbol{p}_h\}, \tag{9}$$

where $[\boldsymbol{T}_s]$ and $[\boldsymbol{T}_p]$ are the respective algebraic transformation matrices.

The moving least square method using superconvergent patch recovery (SPR) technique (Zienkiewicz and Zhu, 1992) originally proposed for stress recovery has been applied to transfer Gauss points variables. The least square procedure is developed on the basis of a standard FE approximation technique. It is assumed that the transferred scalar variable τ over the patch p surrounding the particular assembly points is described by the same order polynomial function as that present in the shape functions of the finite element. This polynomial expansion used for each stress component may be written as:

$$\tau(\boldsymbol{x}) = \big[\boldsymbol{P}(\boldsymbol{x})\big][\boldsymbol{a}], \tag{10}$$

where $[\boldsymbol{P}]$ contains the appropriate polynomial terms and $[\boldsymbol{a}]$ is a set of unknown parameters. For our case in which the bilinear quadrilateral elements are used $[\boldsymbol{P}(\boldsymbol{x})]$ = [1, x, y, xy] and $[\boldsymbol{a}] = [a_1, a_2, a_3, a_4]$.

The determination of the unknown parameters $[\boldsymbol{a}]$ of the expansion given in equation (10) is made by ensuring a least square fit of this to the set of Gauss points existing in the finite element patch considered. In our operation procedure, the transfer transformation (8) gives the stress value ${}^{tr}\tau^i_{h+1}(\boldsymbol{x}^i_{Gh+1})$ specified in the single Gauss point i of the new mesh $h+1$ with the stress vector $\{{}^{tr}\boldsymbol{\tau}^p_h(\boldsymbol{x}^p_{Gh})\}$ composed by the stress values in the Gauss points of the finite element patch p:

$${}^{tr}\tau^i_{h+1}(\boldsymbol{x}^i_{Gh+1}) = [\boldsymbol{T}_s]\big\{{}^{tr}\boldsymbol{\tau}^p_h(\boldsymbol{x}^p_{Gh})\big\}, \tag{11}$$

where $\boldsymbol{x}^i_{Gh+1}$ and $\boldsymbol{x}^p_{Gh}$ are the co-ordinates of Gauss points. A transformation matrix is obtained by a standard least square minimization procedure employing a polynomial

expression (10):

$$[\boldsymbol{T}_s] = \left[\boldsymbol{P}(\boldsymbol{x}^i_{Gh+1})\right]\left([\widetilde{\boldsymbol{P}}]^{\mathrm{T}}[\widetilde{\boldsymbol{P}}]\right)^{-1}[\widetilde{\boldsymbol{P}}]^{\mathrm{T}}. \tag{12}$$

Here, $[\widetilde{\boldsymbol{P}}] \equiv [\widetilde{\boldsymbol{P}}(\boldsymbol{x}^p_{Gh})]$ is a singular rectangular matrix composed of the same polynomial expressions (10) defined at the Gauss points of the patch in the old mesh h. The above procedure (10-11) is also applied to a hardening parameter χ. Matrix $[\widetilde{\boldsymbol{P}}]$ is the same for each component of a transferred variable and hence only a single evaluation of the inverse matrix for the patch is necessary.

For the transfer of the node variables a simple interpolation method has been used. In our operation procedure, the transfer transformation (9) gives the pressure value ${}^{tr}p^i_{h+1}(\boldsymbol{x}^i_{Nh+1})$ specified in the nodal point i of the new mesh $h+1$ with the pressure vector $\{{}^{tr}\boldsymbol{p}^e_h(\boldsymbol{x}^e_{Nh})\}$ composed of the pressure values in the nodal points of the finite element e:

$${}^{tr}p^i_{h+1}(\boldsymbol{x}^i_{Nh+1}) = [\boldsymbol{T}_p]\left\{{}^{tr}\boldsymbol{p}^e_h(\boldsymbol{x}^e_{Nh})\right\}, \tag{13}$$

where $\boldsymbol{x}^i_{Nh+1}$ and $\boldsymbol{x}^e_{Nh}$ are the co-ordinates of nodal points. A transformation matrix is obtained by direct application of a polynomial expression (10):

$$[\boldsymbol{T}_p] = \left[\boldsymbol{P}(\boldsymbol{x}^i_{Nh+1})\right]\left[\bar{\boldsymbol{P}}(\boldsymbol{x}^e_{Nh})\right]^{-1}. \tag{14}$$

The main difference of interpolation compared to the least square approximation is that a set of unknown parameters $[\boldsymbol{a}]$ is uniquely defined in the finite element considered, while $[\bar{\boldsymbol{P}}(\boldsymbol{x}^e_{Nh})]$ is a nonsingular square matrix composed of the same polynomial expressions (10) defined at the nodal points of the element in the old mesh h.

The developed moving least square and interpolation methods are illustrated in Fig. 5. The transfer operation using the moving least square method consists of the following steps: constructing the patches from the Gauss points of the old elements mesh (Fig. 5a), finding the patch where the Gauss point of the new element is (Fig. 5b), transferring the variables from the Gauss points of the old mesh to the Gauss points of the new mesh using the polynomial function (Fig. 5c). The interpolation operation is a similar, but more simple procedure (Fig. 5d).

The proposed remeshing as regeneration of the mesh together with the transfer of the state variables to a new mesh is implemented as post-processor type software compatible with conventional FE codes, while current investigation is implemented into ABAQUS (1998) environment.

The total incremental coupled non-linear FE analysis with the combined remeshing technique comprises a loop of operations until the required overall penetration has been reached. The flow chart of the analysis is presented in Fig. 6. In the case of homogeneous medium a transfer procedure is simplified by omitting the nodal transfer of the pore pressure procedure (9).

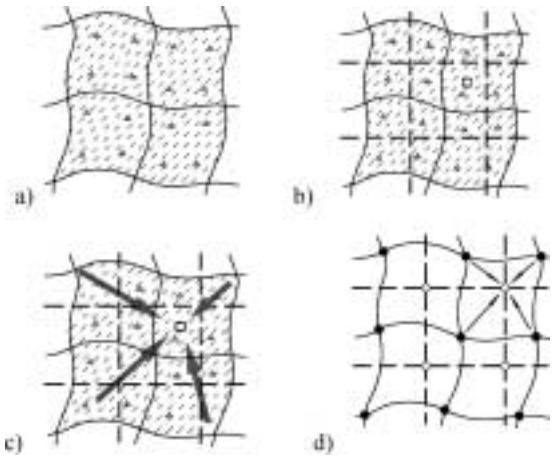

Fig. 5. Transfer operation: moving least square method (a–c) and interpolation method (d).

———	Old deformed mesh	— — —	New unformed mesh
△	Gauss point of old mesh	□	Gauss point of new mesh
•	Nodal point of old mesh	○	Nodal point of new mesh

5. Numerical Results and Discussion

Numerical results given below presents a number of examples illustrating the basic features of the considered remeshing technique capturing finally the non-linear behavior of porous solid with respect to different permeability.

Example 1 – *cylindrical cavity expansion*. The penetration problem can be treated as the expansion of the cylindrical cavity on the shaft of the penetrometer and the expansion of the spherical cavity on the tip of penetrometer (Lunne *et al.*, 1997). The constant cylindrical expansion presents a more simple part of the cone penetration problem, the consideration of which, however, may be used for understanding its role in the entire behavior of penetration as well as for evaluating the role of remeshing.

The cylindrical expansion was treated numerically by considering an example of fixed 2D axisimetric solution domain. The cavity was expanded from 0 to 20 mm radius by controlling the radial motion of the inner boundary. The solution domain (1.0 m in the radial direction and 0.1 m in height) was discretised in the 200 four-noded rectangular elements which form a relatively rough mesh. Such a mesh was taken to increase a possible error of remeshing technique because it is clear that with the finer mesh the diffusion from transferring procedure can only decrease. The problem presents a particular case of a boundary moving with constant velocity, therefore, remeshing should efficiently capture mesh deformation.

The large displacement problem of axisymetric cavity expansion is analyzed in an uncompressible elastic perfectly plastic Mises material. The material has the following properties: yield stress σ_y = 40 kPa, Young's modulus E = 30 MPa and Poisson's ratio $\upsilon = 0.495$.

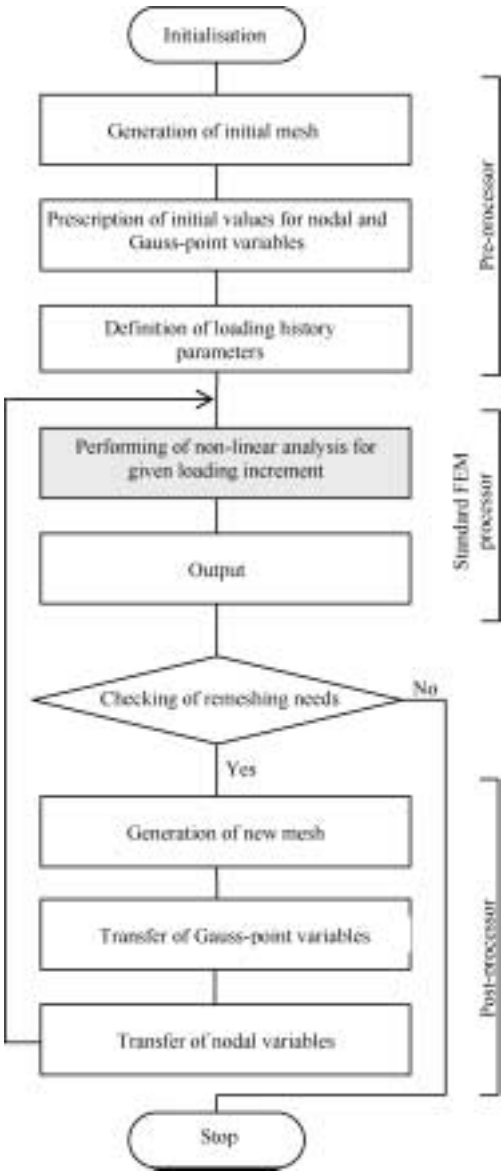

Fig. 6. Flow chart of non-linear coupled FE analysis with moving locally predefined remeshing.

First, one simulation was made without remeshing and two simulations were performed with remeshing: (a) with 4 remeshing steps (per 5 cm of the expansion value); and (b) with 8 remeshing steps (per 2.5 cm of the expansion value). It is apparent that all three numerical results agree extremely well.

On the other hand, remeshing may be treated as iterative approximation of geometrical nonlinearity by geometrically linear models. This approach has already been applied by

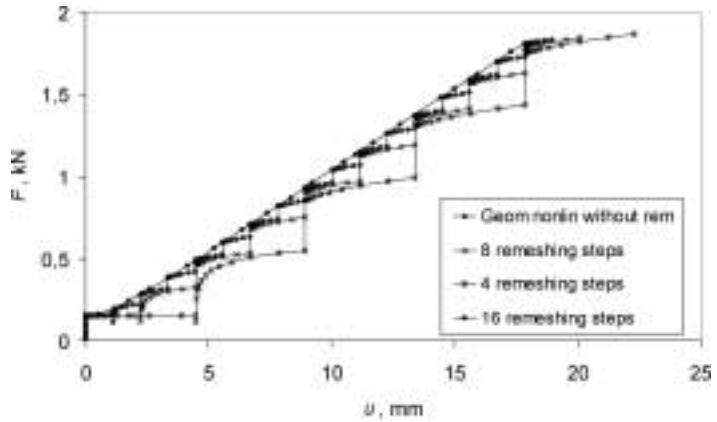

Fig. 7. Resultant expansion force-displacement curves of cavity expansion.

Hu *et al.* (1999). To verify this approach, the small strain analysis with remeshing was performed. Three simulations with 4, 8 and 16 remeshing steps during cavity expansion were made (Fig. 7). It is clearly seen that when more remeshing steps are used the results from small strain FE analysis converge toward the results from geometrically nonlinear FE analysis.

The performed cavity expansion analyses demonstrate that there is no significant drift in the accuracy of the large displacement solution, due to repeated remeshing, while even a linear model with remeshing converges to nonlinear response. The reason of the observed performance of the geometrically nonlinear model is a character of deformation where one side expansion is predominant and small distortions of the elements occur. The results illustrate good performance of remeshing and, at the same time, show that the main difficulties in simulation of penetration occur not due to overall cavity expansion but due to the local expansion of a moving cone. The mesh regeneration rule used for the cavity expansion is further utilized for the CPT problem.

Example 2 *– an illustration of basic features.* This example illustrates basic features of the developed MLP remeshing for the penetration problem. The standard penetrometer was modeled as a rigid surface having a small rounded-off radius r = 2 mm. The cone is placed into a pre-bored hole having the initial depth h = 0.55 m. The size of the FE domain was taken equal to D = 0.625 m, $h + H$ = 1.25 m. The characteristic size of the locally predefined mesh a = 105 mm (Fig. 4). The kinematic boundary conditions are imposed on the medium-medium boundary of a discretised domain. The motion of the bottom boundary was assumed to be restricted in the vertical direction, while the right lateral boundary was restricted in horizontal direction. The initial state of the medium is defined by the weight $\gamma = 18$ kN/m^3 and the lateral pressure ratio K_0 = 1.0. This example deals with a smooth cone exposing the perfectly sliding contact surface, where absolute displacements and velocities of the solid and the boundary may be differ. The homogeneous material is assumed to be elastic-perfectly plastic incompressible Mises material with Young's modulus $E = 30$ MPa, Poisson's ratio $\nu = 0.495$ and the yield stress σ_y

= 40 kPa. The composition of the locally predefined background mesh is illustrated in Fig. 8a. The displacement increment between remeshing steps was taken to be about half the size of the element on the cone.

The simulation results are illustrated by the loading curve $F - u$ (Fig. 9) describing deep penetration of the cone. To investigate the influence of mesh density, four tests using various meshes with 458, 1632, 3541 and 6472 elements, with 4, 8, 12 and 16 elements on the cone tip, respectively, have been performed. The cone penetrated the medium until the displacement of one cone diameter was reached.

The curves obtained by the MLP remeshing technique contain jumps, the frequency of which is related to the frequency of remeshing steps. The curve *4FE* corresponding to the simulation with 4 elements on the cone shows the largest jumps while the curve *16FE* obtained in the simulation with 16 elements demonstrates the smallest jumps. It indicates that the size of jumps decrease with increasing the amount of elements.

The convergence of the resistance load by mesh refinement is illustrated in Fig. 10. The results illustrate the reduction of the jumping amplitude while increasing mesh density and the convergence of all three curves. The interpretation of the results shows that jumping has mainly three reasons. The first is related to shifting of the nodal points by

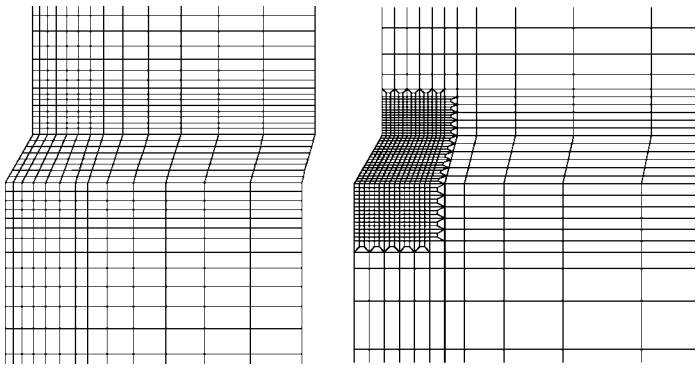

Fig. 8. The locally predefined background mesh used for analysis: a) for homogeneous medium, b) for porous medium.

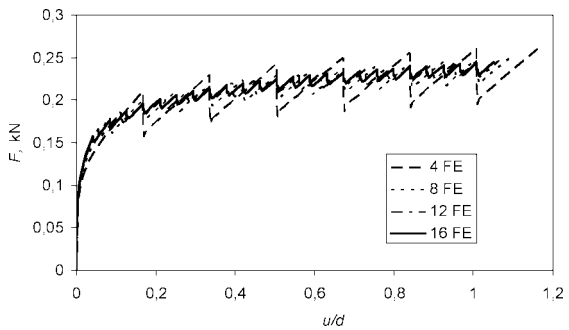

Fig. 9. Loading curve obtained by using different FE discretisation on the cone.

mesh regeneration, the second reason is related to corner node sliding, while the third one is related to a transfer procedure. Since refinement of the mesh and remeshing interval are time-consuming processes, it is desired to reach the equilibrium by a coarser mesh and relatively large remeshing interval. Typical curves of resistance load are presented in Fig. 11. As follows from the convergence test, using different approximation approaches, different smooth loading curves $1, 2$ or 3 may be obtained by the approximation of the simulation results and these curves converge to one curve 2. On the other hand, examination of the results gives an opportunity to construct a smooth curve 2 directly by a coarser mesh and using a relatively large remeshing interval. Finally, it should be emphasized, that the remeshing technique developed and implemented in the post-processor software also comprise the evaluation of the smooth loading curve.

Example 3 – *penetration in homogeneous medium.* The numerical technique discussed and verified above is applied to simulate cone penetration in clay. Since water permeability of clay is very low, the water in this soil has no time to flow out of the pores when cone penetration is performed at the standard speed. Therefore, the cone penetrates the completely undrained soil (Jamiolkowski *et al.*, 1985), and a homogeneous elastic-perfectly plastic incompressible Mises material may be applied for clay (Ukritchon *et al.*, 1998). The contact surface is assumed to be rough (i.e., the limit of friction between the penetrometer and clay is equal to clay shear strength).

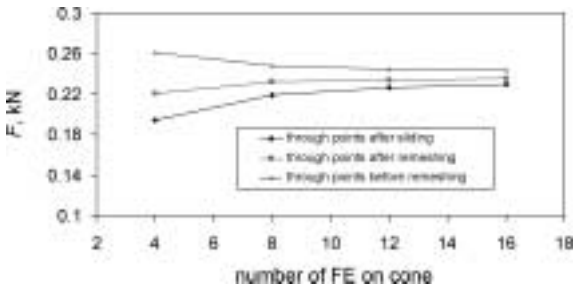

Fig. 10. Convergence of resistance load by mesh refinement.

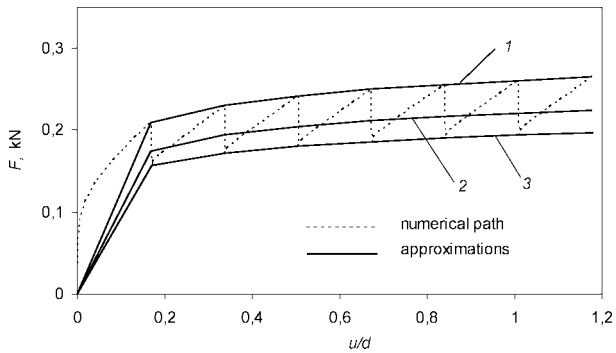

Fig. 11. Loading curve obtained by MLP remeshing technique.

The following material parameters were used: E = 22.5 MPa, $\nu = 0.495, \gamma = 18$ kN/m^3, K_0 = 1.0. As follows from the undrained soil analysis, yield stress σ_y is related to undrained shear strength as$\sigma_y = 2c_u$. Shear strength c_u can be obtained from the triaxial compression test and is taken as c_u = 50 kPa. These parameters define the rigidity index I_r = 150.

After verification by numerical experiments with a larger domain, the size of a discretized domain was taken as $D = 1.1$ m, $h + H$ = 1.8 m. For modeling cone penetration into 5 m depth the upper part of the medium was replaced by the additional external pressure p = 80 kPa on the free upper soil surface. The same boundary conditions and a background mesh as in the previous simulations where used in this example.

The domain was discretized by 1944 bilinear four nodded elements, while soil-cone interaction is described by the contact surface. The total value of DOF of the model is equal to 5082. The cone penetrated up to 14 diameters. The smoothed load-displacement curve illustrating cone behavior is shown in Fig. 12.

Quantitative properties are illustrated by a comparison with experimental results, where the cone factor N_c is used a as quality indicator. It relates cone resistance and material properties. Kurup *et al.* (1994) have presented the results of a calibration chamber study on CPT in overconsolidated cohesive soils giving an average value N_c = 15. The Mises model used here corresponds only to lightly overconsolidated clays. Therefore, the numerically obtained values for the rough cone N_c = 14.4 may be considered as

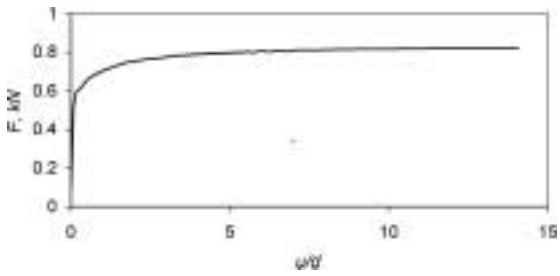

Fig. 12. The loading curve illustrating cone penetration in clay as homogeneous medium.

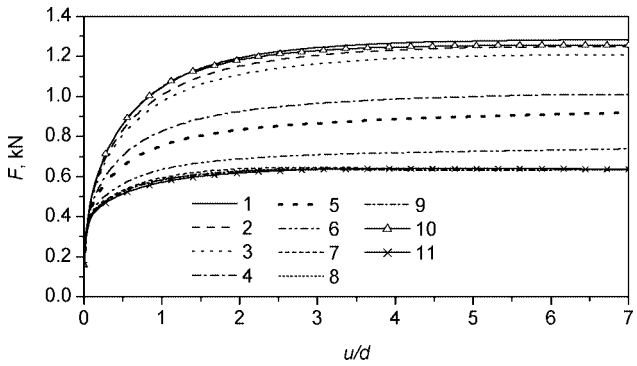

Fig. 13. The loading curve illustrating cone penetration in porous medium.

being in very good agreement with experimental results.

Numerical results prove that the applied remeshing allows us to simulate practically unlimited penetration illustrating the qualitative power of the suggested technique, while the comparison of the results with the experiments quantitatively shows the accuracy of the applied numerical technique.

Example 4 – *penetration in porous medium.* The last example is aimed to illustrate the performance of MLP remeshing technique for cone penetration into porous medium presenting water saturated normally consolidated soil. The friction between a rigid surface and soil was not taken into account, which is a case of the smooth penetrometer. A medium-medium boundary described by the infinite FE was taken on the right side of the discretized domain. It allowed us to reduce the size of the FE domain D to 0.625 m. The vertical size $h + H$ was taken to be 1.8 m.

Since deep penetration is considered and only a limited area around the cone is modeled by finite elements, the gradient of the vertical stress from soil weight and pore water is of minor importance and a homogeneous initial state of stress and pore pressure can be introduced into the model at the start of analysis $\sigma_{v,0}$ = $\sigma_{h,0}$ = 80 kPa, p_0 = 80 kPa.

For normally consolidated soil the modified Drucker-Prager/Cap model (DPC) (ABAQUS, 1998) with the following major parameters is used to describe the properties of the skeleton: Young's modulus E = 5 MPa, Poisson's ratio $\upsilon = 0.2$, friction angle $\phi = 30^\circ$, initial hydrostatic compression yield stress $p_{b,0}$ = 80 kPa. The cap hardening law is defined by the piecewise linear function relating the hydrostatic compression yield stress, p_b, and the corresponding volumetric plastic strain, ε_{vol}^{pl}, as follows: 10 kPa – 0.0, 300 kPa – 0.0005, 500kPa – 0.0023, 1000 kPa – 0.004, 1500 kPa – 0.0052.

The background mesh with 18 elements on the cone was used in simulation, which is far enough for obtaining the accurate results in homogeneous media (Markauskas *et al.*, 2003; Voyiadjis and Abu-Farsakh, 1997), is shown in Fig. 8b. The entire soil domain was discretized using a structured mesh with 1378 bilinear four nodded elements, while soil-penetrometer interaction was described by the contact surface. This mesh provides a high quality solution to a coupled problem leading to minimal pore pressure oscillations in the worst case with a very small water permeability value. Stresses and plastic strains are transferred by moving least square method, while pore pressure is transferred by interpolation method. In our investigation, simulation was limited to the displacement value $u = 260$ mm or relative value $u = 7d$ with respect to cone diameter d.

The validity of remeshing is justified by comparing the simulation results in porous media described by the coupled model (4) and homogeneous media. For the sake of comparison, the cone penetration analysis in fully undrained and fully drained soil as homogeneous medium is made. The modeling results show that in limit cases the differences between the porous media and the homogeneous media are small, which confirms the validity of the remeshing technique for the coupled model. The analysis using different soil permeability values is presented in Fig. 13. The curves from *1* to *9* describe porous media with different permeability (*1* – $k = 10^{-5}$ m/s, *2* – $k = 10^{-6}$ m/s, *3* – $k = 5 \cdot 10^{-7}$ m/s, *4* – $k = 10^{-7}$ m/s, *5* – $k = 5 \cdot 10^{-8}$ m/s, *6* – $k = 10^{-8}$ m/s, *7* – $k = 10^{-9}$ m/s, *8* – $k = 10^{-10}$ m/s, *9* – $k = 10^{-11}$ m/s), while the curves *10* and *11*

present homogeneous media. The character of curves from the analysis proves that the developed remeshing technique provides high quality modeling of deep penetration into the porous media, since the steady-state behavior is reached and subsequently followed with practically unlimited penetration of the cone. It can be seen that cone resistance obtained from the numerical simulations increases rapidly until it reaches the steady state conditions at a depth of about 2*d*, when soil permeability is 10^{-11} m/s, while the steady state is reached at the depth of about 4*d*, when permeability is $k = 10^{-5}$ m/s. When soil permeability is 10^{-11} m/s, the obtained cone resistance is about two times lower than that found for soil permeability of 10^{-5} m/s.

It may be concluded that no excess pore pressure is generated and cone penetration at standard speed is performed in drained conditions when the coefficient of permeability is higher than 10^{-5} m/s. The result obtained is in good agreement with the conclusion made by van den Berg (1994). But in the considered case, the generated excess pore pressure does not affect cone resistance considerably, when soil permeability is greater than 10^{-6} m/s. The fully undrained condition is achieved when permeability is lower then 10^{-10} m/s, but the increase of permeability does not affect cone resistance considerably when permeability is lower than 10^{-9} m/s. Cone penetration in intermediate soils is performed under partially drained conditions. According to their character of the curve and permeability thresholds agree well with the numerical results obtained and discussed by Song *et al.* (1999).

The profiles of the pore pressure and vertical normal stress corresponding to permeability values 10^{-7} m/s and $5{\cdot}10^{-7}$ m/s for penetration depth of $6d$ are depicted in Fig. 14 and 15. The change of pore pressures and vertical normal stresses clearly indicate the change of physical nature of porous medium and the steepest degradation of cone

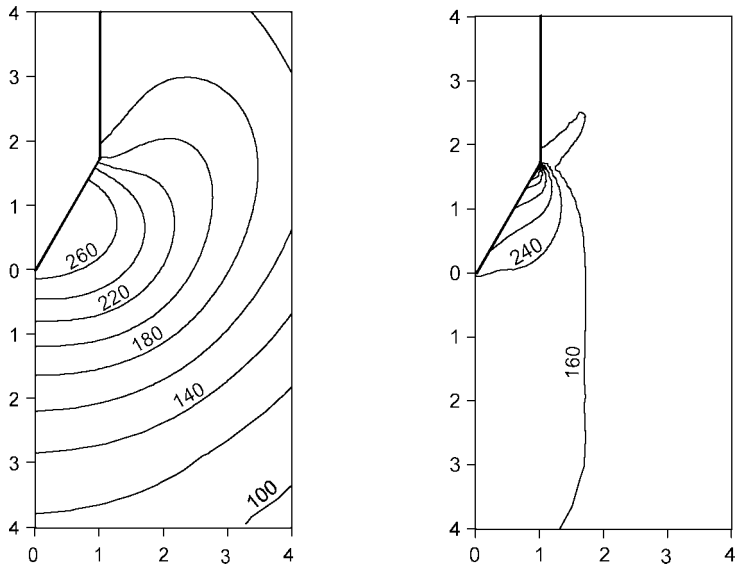

Fig. 14. Pore pressure and vertical normal stress corresponding to permeability $k = 10^{-7}$ m/s.

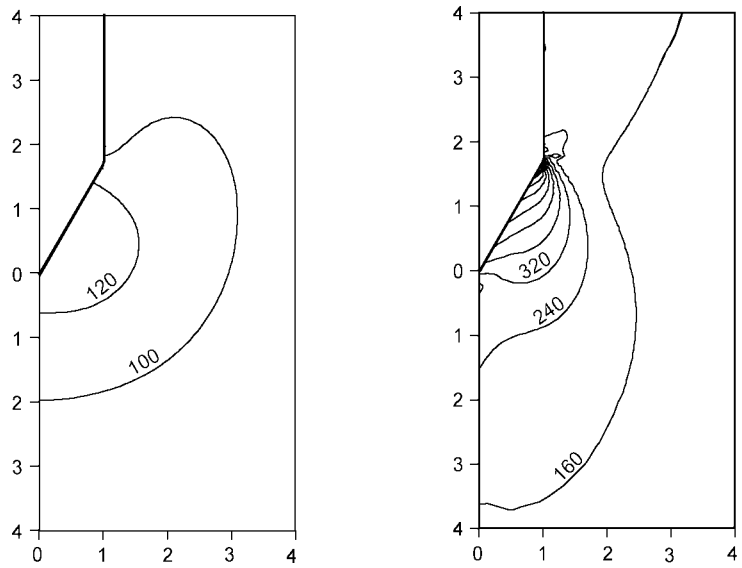

Fig. 15. Pore pressure and vertical normal stress corresponding to permeability $k = 5{\cdot}10^{-7}$ m/s.

resistance, when permeability increases from 10^{-7} m/s to $5{\cdot}10^{-7}$ m/s. Such a sudden change of the generated pore pressure causes a significant change in the loading curve.

Finally, it may be concluded that the developed remeshing technique yields physically reliable results and make possible to investigate the cone penetration in porous medium in a wide range of permeability.

6. Discussion and Conclusions

The moving locally predefined finite element remeshing technique for simulation of rigid cone penetration into homogeneous and porous media using the Lagrangian approach is developed. It involves the transfer operation combining both the moving least square method based on SPR technique and the interpolation method for transfer of state variables. The developed remeshing technique is implemented into post-processor type software compatible with the standard FEM code.

On the basis of the numerical analysis the following conclusions have been drawn:

1. Large distortion of the finite elements and overlapping of the contact surfaces is a serious obstacle in the application of the conventional displacement finite element method to large displacement analysis, but the developed MLP remeshing is able to overcome numerical difficulties coused by large distortions of the initial mesh and by contact sliding and to capture the steady-state penetration behavior.
2. Remeshing technique is supplied with an approximation procedure, which allows the construction of a smooth loading curve by relatively coarse finite element discretisation and remeshing frequency.

3. The developed remeshing technique is applied to the rough cone test in clay, where large penetration of penetrometer $u = 14d$ is reached. The obtained cone factor value 14.4 provides good agreement with experimental results and proves the high quality of the remeshing technique.
4. The developed remeshing technique is applied to modeling deep penetration of rigid penetrometer into elasto-plastic saturated porous media, which is a very difficult or insolvable problem using standard FE software. It exposed good performance in reaching steady-state behavior, with the practically unlimited value of cone displacement. In the present investigation, the simulation was stopped at the displacement value $u = 260$ mm or relative value $u = 7d$ with respect to penetrometer diameter d.
5. The developed remeshing technique combining different approximation of stress and pressure fields demonstrates its ability to capture the behavior of porous media a wide range of permeability and deep cone penetration values. It extends the performance of standard FE software by considering penetration problems which can hardly be solved by a conventional fixed mesh Lagrangian approach.
6. The moving locally predefined remeshing technique is a universal computational tool generally compatible with different formulations and may be applied to other problems, but further research and verification of technical remeshing details are required for particular cases.

Acknowledgement

Financial support of the German Academic Exchange Service for this investigation partially performed in TU Darmstadt is gratefully acknowledged.

References

ABAQUS/Standard (1998). *User's Manuals*. Version 5.8, Habbitt, Karlsson & Sorensen, Inc.

Alves, M.L., J.L.M. Fernandes, J.M.C. Rodrigues and P.A.F. Martins (2003). Finite element remeshing in metal forming using hexahedral elements. *Journal of Materials Processing Technology*, **141**, 395–403.

Bathe, K.J. (1982). *Finite Element Procedures*. Prentice-Hill, Englewoods Cliffs.

Baušys, R., P. Hager and N.E. Wiberg (2001). Postprocessing techniques and h-adaptive finite element-eigenproblem analysis. *Computers & Structures*, **79**, 2039–2052.

Bouchard, P.O., F. Bay and Y. Chastel (2003). Numerical modelling of crack propagation: automatic remeshing and comparison of different criteria. *Comput. Methods Appl. Mech. Engrg.*, **192**, 3887–3908.

Belytschko, T., W.K. Liu and B. Moran (2001). *Nonlinear Finite Elements for Continua and Structures.* John Wiley & Sons.

Chand, C., R. Kumar (1998). Remeshing issues in the finite element analysis of metal forming problems. *Journal of Materials Processing Technology*, **75**, 63–74.

Chenot, J.L., and F. Bay (1998). An overview of numerical modelling techniques. *Journal of Materials Processing Technology*, **80–81**, 8–15.

Crisfield, M.A. (1997). *Non-linear Finite Element Analysis of Solids and Structures*, vol. 2. Wiley, Chichester.

Diez, P., and A. Huerta (1999). A unified approach to remeshing strategies for finite element h-adaptivity. *Comput. Methods Appl. Mech. Engrg.*, **176**, 215–229.

Erhart, T., L. Taenzer, R. Diekmann, W.A. Wall (2001). Adaptive remeshing issues for fast transient highly nonlinear processes. In *Proceedings of European Conference on Computational Mechanics, ECCM-2001*, Vol. on CD-ROM.

Gautham, B.P., S. Goyal and A. Gandhe (2003). Boundary controlled automatic remeshing for 2D simulation of metal forming. *Journal of Materials Processing Technology*, **134**, 108–114.

Hu, Y., and M.F. Randolph (1998). Deep penetration of shallow foundation on non-homogeneous soil. *Soils and Foundations*, **38**(1), 241–246.

Jamiolkowski, M., C.C. Ladd, J.T. Germaine, R. Lancellotta (1985). New developments in field and laboratory testing of soils. In *Proceedings of the Eleventh ICSMFE*, vol. 1. A.A.Balkema, Rotterdam. pp. 57–153.

Karakouzian, M., B. Avar, N. Hudyma, J. Moss (2003). Field measurements of shear strength of an underconsolidated marine clay. *Engineering Geology*, **67**, 233–242.

Kurup, P., G. Voyiadjis, M. Tumay (1994). Calibration chamber studies of piezocone test in cohesive soils. *J. of Geotechnical Engineering*, ASCE, **120**(1), 81–107.

Lee, C.K., and R.E. Hoobs (1999). Automatic adaptive finite element mesh generation over arbitrary two-dimensional using advanced front technique. *Computers & Structures*, **71**, 9–34.

Lee, G.A., D.Y. Kwak, S.-Y. Kim and Y.T. Im (2002). Analysis and design of flat-die hot extrusion process. 1. Three-dimensional finite element analysis. *Int. J. of Mechanical Sciences*, **44**, 915–934.

Liu, D., Z.J. Luo, and M.X. Gu (1998). The algorithm of automatic local mesh subdivision and its application to finite-element analysis of a large deformation forming process. *Journal of Materials Processing Technology*, **83**, 164–169.

Liyanapathirana, D.S., A.J. Deeks and M.F. Randolph (2000). Numerical modeling of large deformations associated with driving of open-ended piles. *Int. J. for Numerical and Analytical Methods in Geomechanics*, **24**, 1079–1101.

Lunne, T., P.K. Robertson and J.M. Powell (1997). *Cone Penetration Testing in Geotechnical Practice*. Blackie Academic & Professional, London.

Mabsout, M., L. Reese, J. Tassoulas (1995). Study of pile driving by finite-element method. *J. Geotechnical Engineering*, ASCE, **121**(7), 535–543.

Markauskas, D., R. Kačianauskas, M. Šukšta (2002). Modeling the cone penetration test by the finite element method. *Foundation of Civil and Environmental Engineering*, **2**, 125–140.

Markauskas, D., R. Kačianauskas and R. Katzenbach (2003). Numeric analysis of large penetration of the cone in undrained soil using FEM. *Journal of Civil Engineering and Management*, **9**(2), 122–131.

Markauskas, D. (2003). Modeling of the cone penetration testing using finite element method. *PhD thesis*, VGTU (in Lithuanian).

Owen, S.J., and S. Saigal (2000). Surface mesh sizing control. *Int. J. for Numerical Methods in Engineering*, **47**, 497–511.

Pedersen, T. (1998). Remeshing in analysis of large plastic deformations. *Computers & Structures*, **67**, 279–288.

Peric, D., Ch. Hochard, M. Dutko and D.R.J. Owen (1996). Transfer operators for evolving meshes in small strain elasto-plasticity. *Comput. Methods Appl. Mech. Engrg.*, **1**(37), 331–344.

Potts, D., and L. Zdravkovic (1999). *Finite Element Analysis in Geotechnical Engineering*, Volume I – Theory. Telford Publishing, London.

Sheng, D., K. Axelsson, O. Magnusson (1997). Stress and strain fields around a penetrating cone. In *Proc. VI Int. Symposium on Numerical Models in Geomechanics/NUMOG VI*. A.A. Balkema, Rotterdam.

Song, C.R., G.Z. Voyiadjis and M.T. Tumay (1999). Determination of permeability of soils using the multiple piezo-element penetrometer. *Int. J. Numer. Anal. Meth. Geomech*., **23**, 1609–1629.

Susila, E., and R. Hryciw (2003). Large displacement FEM modeling of the cone penetration test (CPT) in normally consolidated sand. *Int. J. Numer. Anal. Meth. Geomech*., **27**, 585–602.

Ukritchon, B., A.J. Whittle, S.W. Sloan (1998). Undrained limit analyses for combined loading of strip footings on clay. *Journal of Geotechnical and Geoenvironmental Engineering*, ASCE, **124**(3), 265–276.

Van den Berg, P. (1994). *Analysis of Soil Penetration*. PhD Thesis, Delft University of Technology, Netherlands.

Vasiliauskienė, L., and R. Baušys (2002). Intelligent initial finite element mesh generation for solutions of 2D Problems. *Informatica*, **13**(2), 239–250.

Voyiadjis, G.Z., and M.Y. Abu-Farsakh (1997). Coupled theory of mixtures for clayey soils. *Computers and Geotechnics*, **20**, 195–222.

Voyiadjis, G.Z., and D. Kim (2003). Finite element analysis of the piezocone test in cohesive soils using an elastoplastic–viscoplastic model and updated Lagrangian formulation. *Int. J. Plasticity*, **19**, 253–280.

Wriggers, P., and A. Rieger (2003). Advances in adaptive methods for thermo-mechanical contact problems. In *CMM-2003 – Computer Methods in Mechanics*; *1st CEACM Conference on Computational Mechanics*, short papers. Gliwice/Wisla, Poland. pp. 17–18.

Yang, Z., and J. Chen (2004). Fully automatic modelling of cohesive discrete crack propagation in concrete beams using local arch-length methods. *Int. J. of Solids and Structures*, **41**(3–4), 801–826.

Zhu, Y.Y., T. Zacharia and S. Cescotto (1997). Application of fully automatic remeshing to complex metal-forming analyses. *Computer & Structures*, **62**(3), 417–427.

Zienkiewicz, O.C. (1984). Coupled problems and their numerical solution. In R.W. Lewis, P. Bettess and E. Hinton (Eds.), *Numerical Methods in Coupled Systems*, John Wiley & Sons Ltd. pp. 35–58.

Zienkiewicz, O.C., and J.Z. Zhu (1992). The superconvergent patch recovery and a posteriori error estimates. Part 1: The recovery Technique. *Int. J. for Numerical Methods in Engineering*, **33**, 1331–1364.

R. Kačianauskas, professor, dr. habil.-eng., a head of the Department of Strength of Materials, senior researcher in the Laboratory of Numerical Modelling, Vilnius Gediminas Technical University, Lithuania. He graduated Vilnius Civil Engineering Institute, now Vilnius Gediminas Technical University (VGTU), Lithuania in 1975, PhD degree obtained in 1982 at VGTU, held DAAD scholarship (Germany) in 1986, 1992 and 2000. Visiting researcher in Sweden, UK, Portugal and Switzerland. Author of monograph "Computer Methods in Multi-Level Modelling of Beams and Shells" and over 100 publications. Research interests comprise computational mechanics, finite element method, fracture mechanics, modelling of structures, materials and multi-physical phenomena.

D. Markauskas has graduated from Vilnius Gediminas Technical University (VGTU) Faculty of Civil. He received the PhD degree from VGTU in 2003. Now he is research feloow in Laboratory of Numerical Modeling. His reseach interests include finite element method, discrete element method for solution of mechanical problems.

Slanki lokaliai apibrėžta baigtinių elementų pergeneravimo technika kūgio formos zondo gilios penetracijos analizei

Rimantas KAČIANAUSKAS, Darius MARKAUSKAS

Aprašoma slanki lokaliai apibrėžta baigtinių elementų tinklo pergeneravimo technika, skirta kūgio formos standaus zondo giliai penetracijai į homogeninę ir poringąją terpę modeliuoti. Ši technika realizuota postprocesoriaus tipo programa suderinama su standartinėmis BEM programomis. Siūloma technika apima ir kintamųjų perkėlimo į skirtingus tinklus operacija, taikant slankiųjų mažiausių kvadratų metodą įtempimams ir interpoliavimo metodą slėgiams perkelti. Pasiūlytas metodas įgalino išvengti skaitinių sunkumų dėl didelio Langranžo tinklo išsikraipymo ir kontaktinio praslydimo, ir taip pasiekti nusistovėjusį būvį modeliuojant kūgio penetraciją į tampriąją plastinę homogeninę, o taip pat poringąją terpę ir įsmeigiant kūgį iki keleto kūgio skersmenų.